JOURNAL OF MATERIALS SCIENCE 19 (1984) 3028–3042

The deformation stress of highly brittle explosive crystals from real contact area measurements

M. MUNAWAR CHAUDHRI
Cavendish Laboratory, Madingley Road, Cambridge, UK

An experimental study is described in which the deformation stress of millimetre-size highly brittle as-grown single crystals of explosive materials has been determined using a novel experimental technique. The technique involves the loading of the test crystal against a transparent glass plate with *in situ* measurements of the real area of contact under load using an optical microscope. For all explosive crystals the deformation stress was found to increase with load reaching a plateau at higher loads. The maximum deformation stress of a crystal was found to be considerably lower than its Vickers diamond hardness value. A discussion on the determination of the uniaxial yield stress of small particles is also given.

1. Introduction

Recently, Chaudhri [1] published a model for the initiation of explosions in compacts of sensitive solid explosives when they are impacted by hard needle-shaped strikers. According to this model, an explosion results due to the high temperatures generated by friction at the contacting surfaces of the explosive particles which are picked up by the striker's tip and carried into the explosive compact. To make reliable quantitative estimates of the temperatures generated at the rubbing surfaces, a knowledge of several physical properties of the particles is needed [1]. One such property of significant importance is the deformation stress of a particle pressed against another with a given normal load. To determine this parameter direct measurements of the real area of contact are required, which are difficult to make even for ductile metals as has recently been pointed out by Tabor [2]. For brittle materials the situation is further complicated by cracking which can occur at quite small loads. Here the results of a novel experimental investigation are reported in which the deformation stress of a number of highly brittle [3, 4] as-grown explosive crystals has been determined from measurements of the real area of contact when they are pressed against a hard transparent surface with a known normal load. In the literature, such a method of determining the deformation stress of brittle crystals of shapes other than the rectangular parallelopiped does not appear to have been reported before.

2. Experimental details

2.1. Materials

Single crystals of lead azotetrazole (LAT) of types A and C were obtained from Dr P. Collins of PERME (UK); type A were of pyramidal shape about 2 mm across, whereas type C were needle-like 1 to 2 mm in length and about 0.5 mm in diameter. Single crystals of α-lead azide were grown in the laboratory by a diffusion method [5]; these were also needle shaped, 0.3 to 0.5 mm in diameter, and 1 to 2 mm in length. Crystals of β-cyclotetramethyl-tetranitramine (β-HMX) and cyclotrimethylenetrinitramine (RDX) were also grown in the laboratory by slow evaporation of a saturated solution in acetone at 70° C. β-HMX single crystals were thick platelets with relatively good edges, whereas crystals of RDX did not show sharp edges and generally had rounded corners. Potassium chloride crystals about 1 cm × 1 cm × 1 cm in size were obtained from BDH (UK), from which pieces about 1 to 2 mm in size were cleaved for these

0022–2461/84 $03.00 + .12

TABLE I Chemical formuli and some crystallographic and mechanical properties of the crystals used in this work

Material	Chemical formula	Crystal class and space group	Primary glide system
α-lead azide (α-PbN_6)	PbN_6	Orthorhombic *Pcmn* [6]	not known
Lead azotetrazole (LAT)			
type A	$[C_2N_{10}Pb]x \cdot H_2O$ (x between 0 and 2)	not known	not known
type C	$[C_2N_{10}Pb] \cdot Pb(OH)_2$	not known*	not known
β-cyclotetramethylene-tetranitramine (β-HMX)	$(CH_2NNO_2)_4$	monoclinic $P2_1/C$ [8]	not known
Cyclotrimethylene-trinitramine (RDX)	$C_3H_6N_3(NO_2)_3$	orthorhombic *Pbca* [9]	(0 1 0) [0 0 1] [10]
Potassium chloride (KCl)	KCl	cubic $Fm3F$ [11]	{1 1 0} ⟨1 $\bar{1}$ 0⟩ [12]

*Melanie A. Pierce-Butler [7] has determined the structure of LAT type D having the same chemical formula as that of the type C; the crystal class is triclinic and space group $P1$.

experiments. Table I lists the chemical formulae of the various explosives along with their crystal structures and slip systems (if known).

2.2. The principle of the experimental technique

The principle of the technique can be illustrated with the help of Fig. 1. In Fig. 1a a light beam is reflected from a partially silvered surface S and hits a polished glass plate normally. If the refractive indices of the glass and air are n_1 and n_2 respectively, then the intensity I_1 of the light reflected from surface A, for unit incident intensity, is:

$$I_1 = \left(\frac{n_1 - n_2}{n_1 + n_2}\right)^2 \quad (1)$$

Substituting $n_1 = 1.5_2$ and $n_2 = 1$, we have $I_1 = 0.04$.

A crystal of the test material is then brought into perfect contact at surface A as shown in Fig. 1b. The intensity I_2 of the light reflected from the glass/crystal interface is then given by:

$$I_2 = \left(\frac{n_3 - n_1}{n_3 + n_1}\right)^2 \quad (2)$$

where n_3 is the refractive index of the crystal. For the crystals used in this work n_3 is in the range 1.5 to 2.6. Taking a value of n_3 of 1.6 (say), $I_2 = 0.0066$, which is considerably smaller than I_1. The same is true for other values of n_3 in the given range. Thus, the reduction in the intensity of the reflected light gives us a convenient method of measuring the area of real contact between a non-metallic crystal and a transparent glass plate.

2.3. The compression apparatus

A schematic diagram of the arrangement used for compressing crystals against an optically flat glass surface and simultaneously measuring the area of

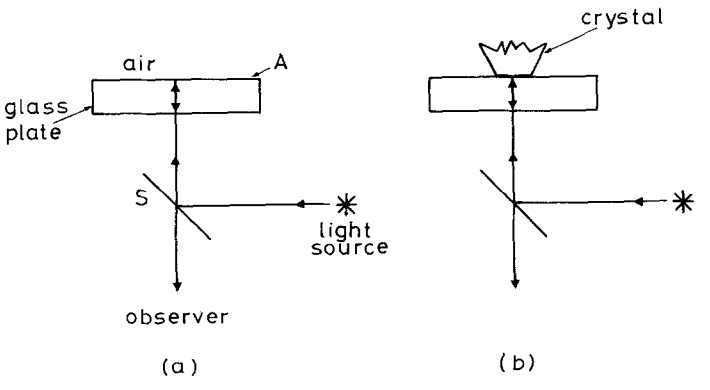

Figure 1 Diagram showing the principle of the experimental technique used for measuring the real area of contact.

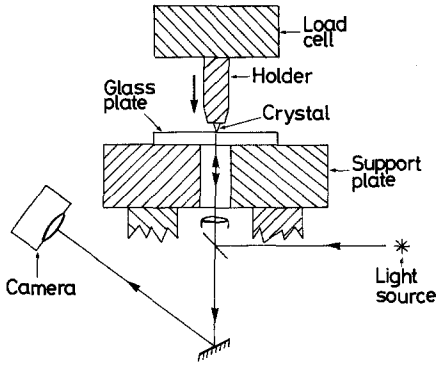

Figure 2 Schematic diagram of the arrangement used for measuring the real area of contact of a crystal loaded against a smooth glass plate.

real contact between the crystal and the glass surface is shown in Fig. 2. The crystal to be examined is mounted on a steel holder with an epoxy "araldite". Before the epoxy hardens, the crystal is carefully positioned so that as far as possible a sharp corner of the crystal is along the axis of the holder, or a sharp edge is normal to it.

The steel holder itself is screwed into a sensitive load cell capable of measuring loads from less than a gramme to several kilogrammes. The load cell is rigidly mounted on the crosshead of a mechanical testing machine (Instron No. 1122); in all experiments the crosshead speed was $0.05\,\text{mm}\,\text{min}^{-1}$. The glass plate is placed on a thick steel support plate and the contact area between the crystal and the glass plate is viewed in reflection using an optical microscope focused on the glass surface, as shown in the figure. When desired, photographs of the contact area are taken, the magnification on the camera film being × 60.

The experimental procedure was as follows. First the crystal was brought to within 5 to 10 μm of the glass surface and a photograph taken. At this stage the field of view was uniformly illuminated. Then the crystal was brought into contact with the glass surface, with the normal load being a gramme or less. It was observed that wherever the crystal made real contact with the glass surface, the intensity of illumination decreased markedly. The load was then further increased by a small amount and another photograph taken. This procedure was continued for several loads and a corresponding sequence of photographs was made.

The maximum load applied on a crystal depended upon its size and the type so that only a minimum amount of cracking occurred. Photographs were also taken during the unloading of the crystal and it was found that in all cases plastic deformation of the crystal had occurred over the entire region in real contact with the glass plate. The deformed region was flat and optically smooth and when the crystal was only just removed from the glass plate the flat gave a mirror-like reflection.

Silhouette optical micrographs of crystals before and after deformation were also taken. Although the deformed regions were relatively small, in some cases the deformation could be clearly seen in the migrographs.

The measurements of the real area of contact were made from enlarged prints using a transparent millimetre grid. In this manner, a real contact area as small as 1 μm × 1 μm could be measured.

3. Results

The results from different crystals are given below separately.

3.1. α-PbN_6

Two single crystals of this material were investigated. Fig. 3a shows the profile of a crystal before it was deformed. It was loaded on an edge (marked with arrow) along the *c*-axis, and the photographs of real contact are shown in Fig. 3b. The load on the crystal in grammes is shown alongside each frame. In the uppermost frame, the crystal has not touched the glass plate and is only a few μm from the surface. Note that the entire field is uniformly illuminated (the black circular spot in the centre of frames 1 and 2 is due to a dust particle). In frame 2, the load has been increased to 10.5 g and a dark band has appeared in the centre. The crystal is in real contact with the glass surface at all points in the band. In the next frame, the load has been further increased to 20 g, and note that the area of the dark band has also increased. The crystal was then unloaded, first to 4 g and then to zero. At 4 g the area of the dark region in the band has decreased as some of it has become brighter than the background. At zero load, the entire band has changed into a bright one. These observations strongly indicate that the crystal is no longer in contact with the glass plate and that the edge of the crystal had plastically deformed to a smooth flat surface.

The crystal was then again loaded and the real areas of contact corresponding to loads of 24, 32 and 41 g are also shown in the figure. As the load

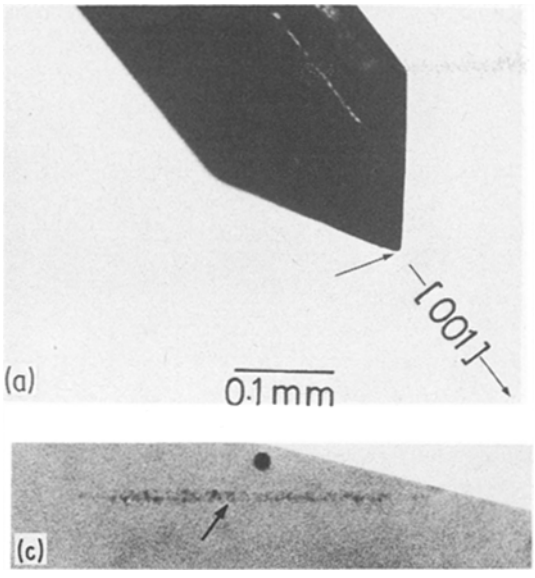

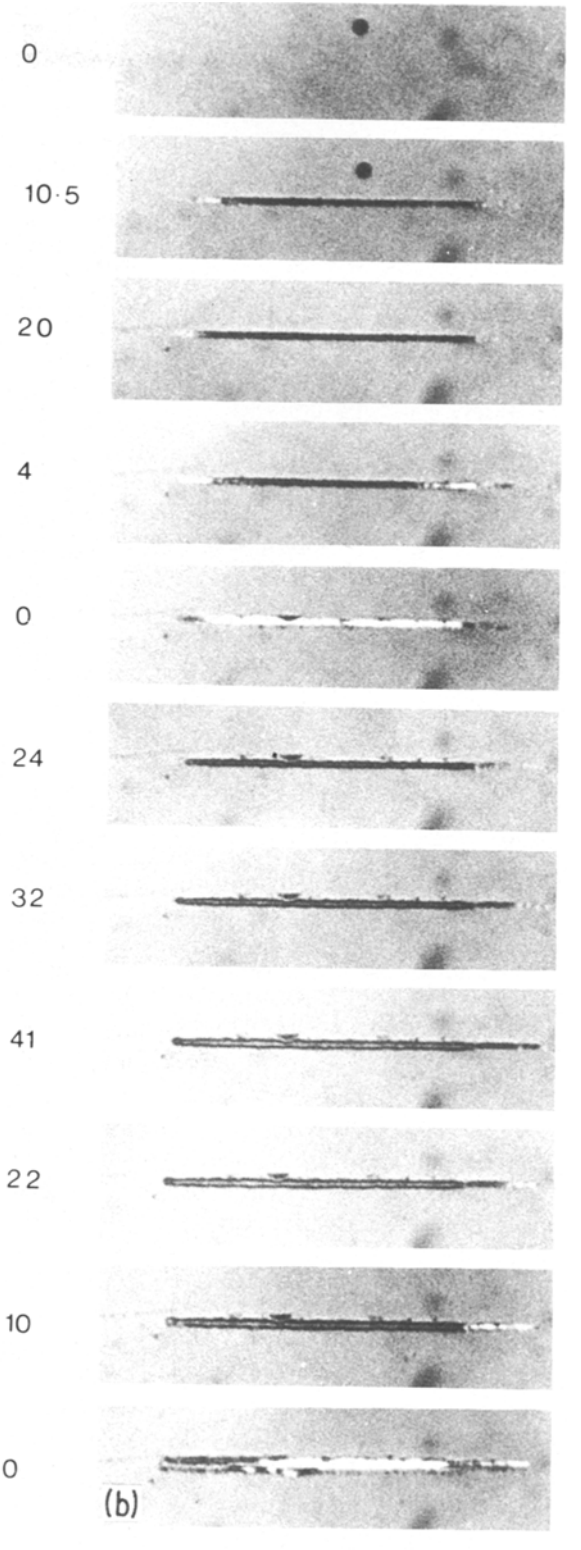

Figure 3 (a) Profile of an α-lead azide single crystal which was loaded along the *c*-axis; the edge before being deformed is indicated by the arrow.

(b) The variation of the real area of contact of the lead azide crystal shown in Fig. 3a when it is compressed by different loads. The figure on the left of each frame is the load (in g) on the crystal. The dark band represents the real contact, whereas the bright band is due to the reflection of the light from the plastically deformed surface when it is only slightly separated from the glass plate.

(c) A layer of particles of lead azide adhered to the glass plate.

increases, both the width and the length of the band increase. For loads above 24 g, a thin bright line appears at the centre of the dark band. At present its origin is not clear. The crystal was then finally unloaded, and during the unloading the area of real contact decreases, as is indicated by the change in the contrast. However, as the crystal has deformed plastically, the decrease is slight initially and only when the crystal is nearly completely separated from the glass at zero load does a pronounced decrease in the area of real contact occur. As already stated, the flat on the crystal forms due to its plastic deformation; it is rather smooth, and can give enhanced illumination only when just separated from the glass plate. The behaviour of the second crystal was found to be quite similar to that of the first.

It should be pointed out here that if a crystal of lead azide was loaded for the first time against the glass surface even by as low a load as 1 g, it left on the glass surface a thin film consisting of very small particles which could not be resolved

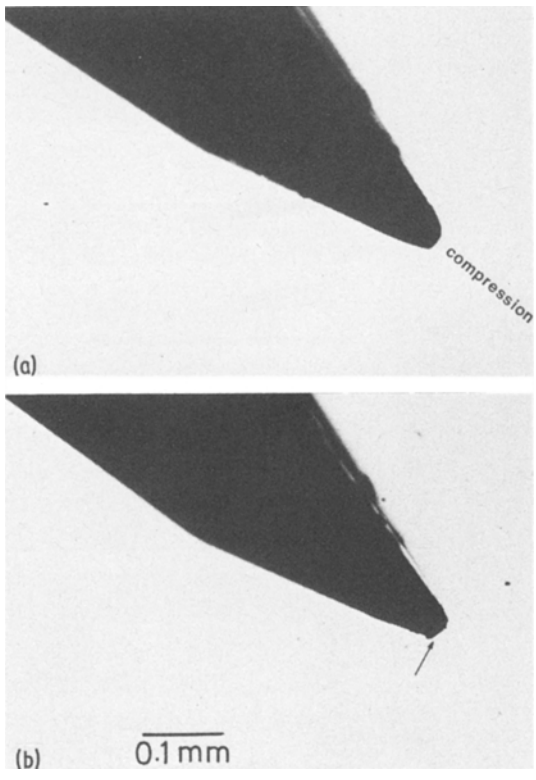

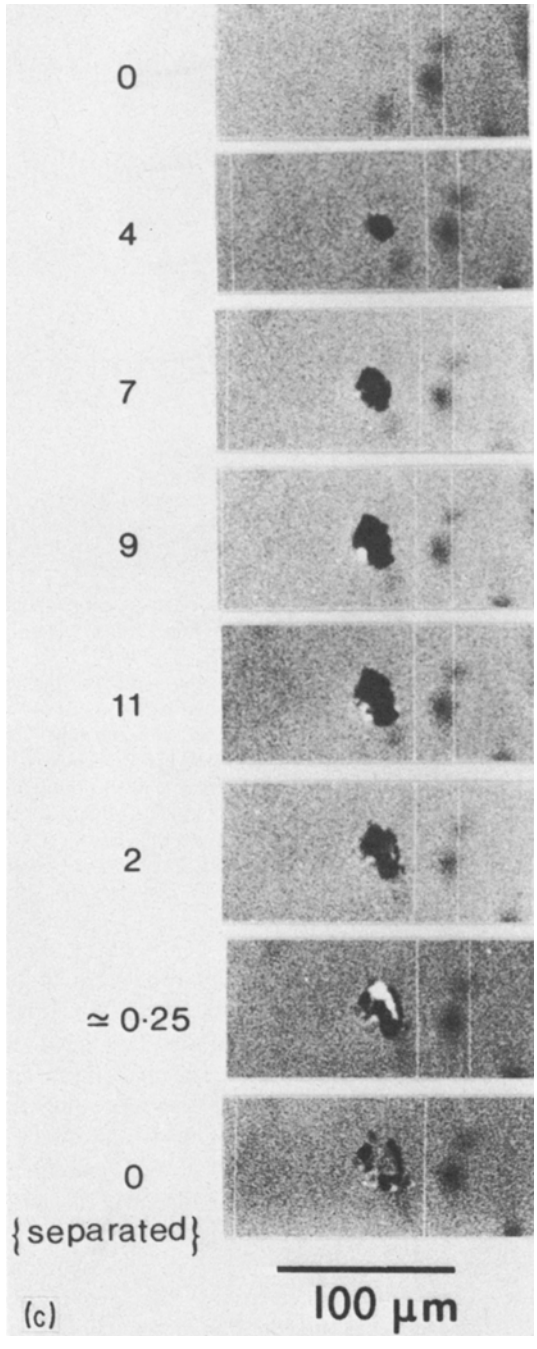

Figure 4 (a) A crystal of LAT type C before being compressed. The edge to be loaded is of a pyramidal shape, with the angles between the pairs of opposite faces being 36° and 81°. (b) After the compression experiment the tip of the crystal was found to be deformed plastically (see at arrow). (c) The variation of the real area of the contact of the LAT crystal shown in Fig. 4a when it is pressed against the glass plate at different loads. The load (in g) on the crystal is shown on the left of each frame. Dark areas represents real contact.

even under a high powered optical microscope. An examination of the film in a scanning electron microscope was not successful either because of the decomposition of the particles by the electron beam. These fine particles are probably of lead azide and an optical micrograph of such a thin film is shown in Fig. 3c.

Another interesting observation was that neither during the approach of a lead azide crystal towards the glass plate nor during the crystal's removal from the plate after having been loaded, were the surface or adhesive forces strong enough to be registered by the load cell. That is, these forces were less than 0.25 g.

3.2. LAT

We examined three crystals of LAT type "C" and only one of LAT type "A". The compression behaviour of type "C" crystals was quite similar and results from a crystal are shown in Fig. 4c. The end of the crystal which was loaded was of pyramidal shape with the angles between the opposite faces being 36° and 81°. Figs. 4a and b show this end before and after deformation, respectively. The region which was loaded is indi-

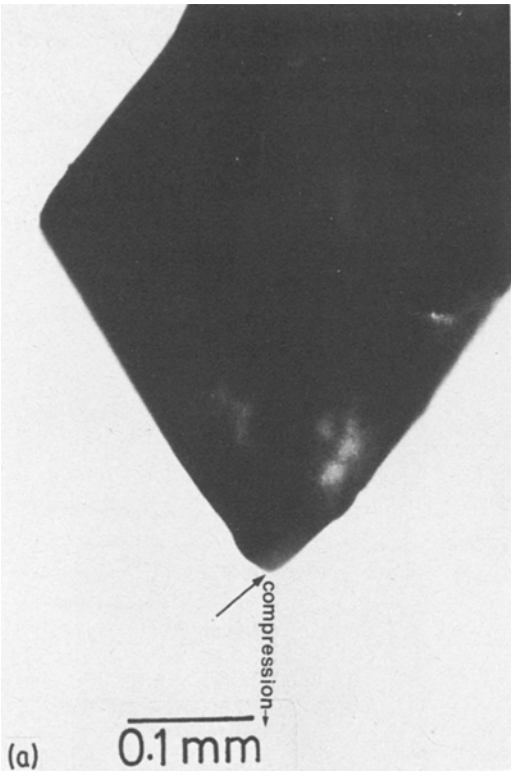

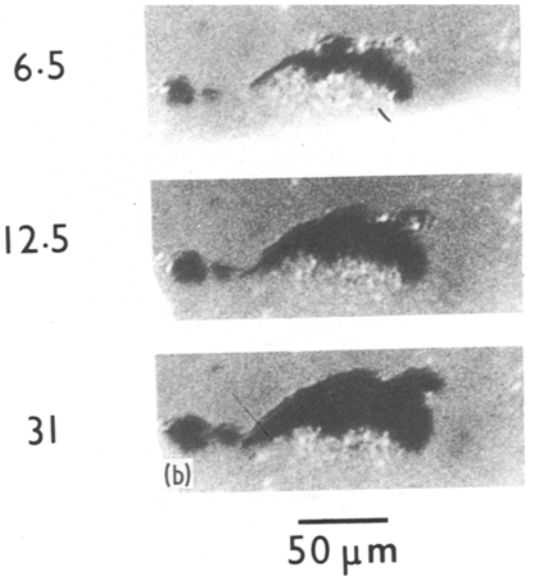

Figure 5 (a) A crystal of LAT type A before being compressed; the loading point is marked with the arrow. (b) The variation of the area of real contact of the LAT type A shown in Fig. 5a when it is compressed against the glass plate at different loads. The load (in g) on the crystal is shown on the left of each frame. Dark areas represent real contact.

cated with an arrow and it is quite clear that plastic deformation of the tip has taken place.

It will be seen from Fig. 4c that as the normal load on the crystal is increased from 0 to 11 g, the area of real contact also increases; in this case, because of the geometry of the loaded zone, the area of real contact is approximately circular. When unloading occurs and the load is reduced to 2 g, the area of real contact only reduces slightly, as in the case of lead azide. When the load is further reduced to 0.25 g, some separation of the surfaces occurs, as is evident from the very bright spot in the middle of the area of contact. When the surfaces are completely separated (i.e. last frame), there are still some dark areas left; these are due to an adhered layer of LAT on the glass surface.

Figs. 5a and b show a crystal of LAT (type A) before being compressed and the variation of real area of contact with load, respectively. As will be seen in Fig. 5a, the corner of the crystal which was loaded was not very sharp with the result that the contact occurs at several isolated areas (see Fig. 5b). Moreover, as for the above two materials, when the load was increased from 6.5 g to 31 g, the area of real contact also increased. On complete unloading, a very thin layer of adhered particles (smaller than 1 μm) was left on the glass plate.

3.3. β-HMX

Two single crystals of this material were investigated, but photographs of the real area of contact of only one of them will be shown here. Fig. 6a shows the face of the crystal that was loaded (this crystal did not have any pronounced corners or sharp edges) and the variation of the area of real contact with load is shown in Fig. 6b; loads in grammes are given at the bottom left-hand corner of each frame. In this case, the real area of contact is not of a regular shape. Moreover, for loads greater than 21.5 g some fringes appear outside the area of real contact. Again, for these crystals the size of the area of real contact increased with load.

The plastic deformation of a sharp corner of the second crystal is clearly illustrated in Fig. 7. Fig. 7a shows the corner of the crystal which was loaded along the *a*-axis. Fig. 7b shows the state of the corner after the crystal had been loaded to 11 g and then unloaded. Note the permanent deformation of the corner, but no cracking is

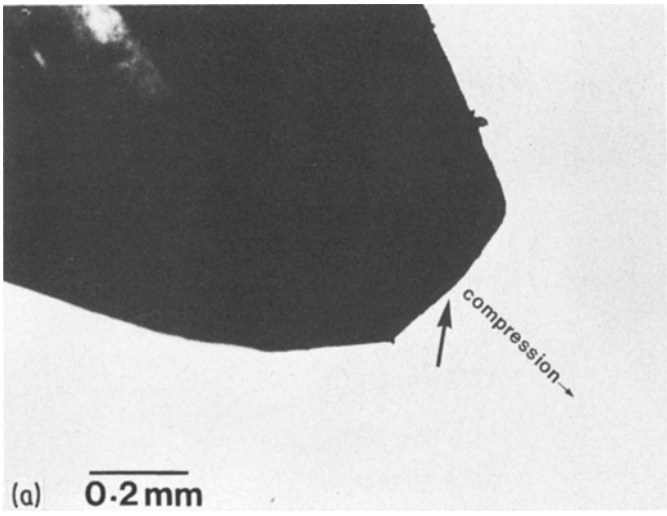

Figure 6 (a) A crystal of β-HMX before being loaded at the region marked with the arrow.

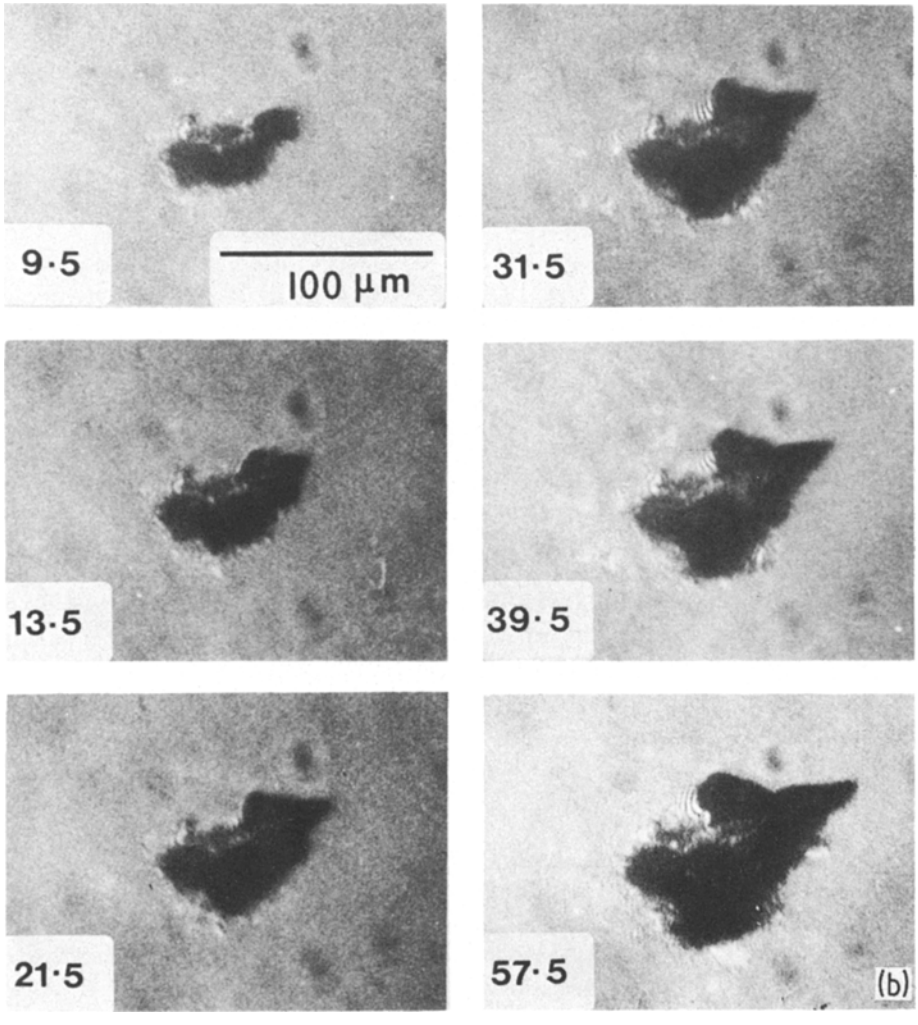

Figure 6 (b) The variation of the area of real contact of the β-HMX crystal shown in Fig. 6a when it is compressed against the glass plate at different loads. The load (in g) on the crystal is shown at the bottom left-hand corner of each frame. Dark areas represent the real contact. Note also the optical interference fringes for the three highest loads; these regions giving interference fringes are not in real contact.

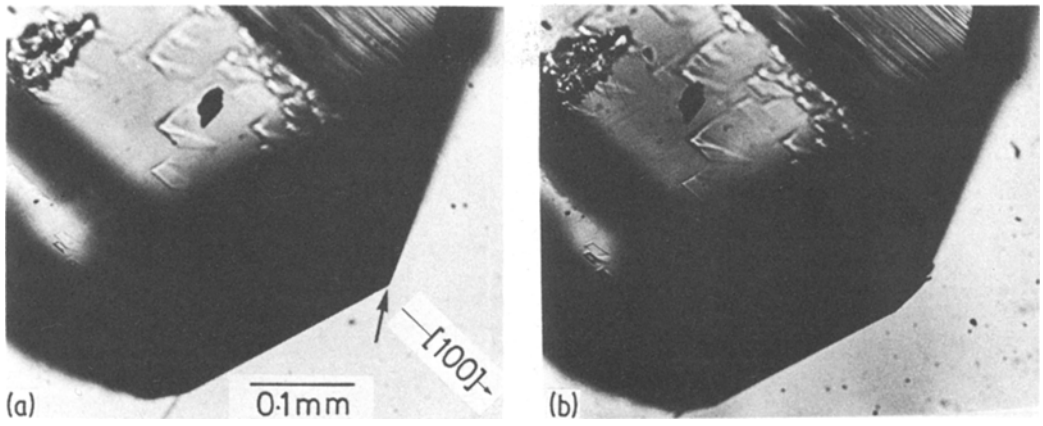

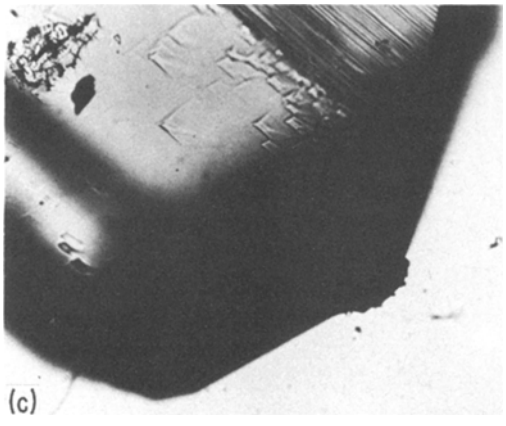

Figure 7 A rather sharp-edged crystal of β-HMX. It was first compressed to a load of 11 g (Fig. 7b) and then to 23 g (Fig. 7c). In both cases, plastic deformation of the crystal tip occurred.

apparent yet. When the crystal was further loaded to 23 g and then unloaded, the volume in which permanent deformation occurred also increased (see Fig. 7c). This frame also indicates that some fracturing of the tip may have occurred. However, it cannot be said with any certainty whether the adhesion of the crystal tip to the glass enhanced the fracture.

It may be added here that a film of adhered fine particles of β-HMX crystals was left on the glass surface even after loading to only 3 g. Whether this film formed at lower loads was not examined.

3.4. RDX

Single crystals of this material were approximately spherical and of diameter less than 1 mm. Two crystals were investigated, but photographs of the area of real contact of only one of them will be shown here. In Fig. 8a the profile of a crystal is shown with an arrow marking the region which was loaded. Fig. 8c shows the variation of the size of the area of real contact with increasing load; the load in grammes is shown at the bottom left-hand corner of each photograph. At zero load the crystal is very close to the glass surface, but not in contact with it. This causes a reflection of the light as is indicated by the lighter area in the frame. As the load is increased to 1.5 g real contact occurs at the point indicated by the arrow and the intensity of the reflected light decreases giving a darker zone. Because of the rough nature of the crystal surface the contact occurs at several isolated zones as is clearly indicated by frames corresponding to higher loads. This sequence gives a clear example of the asperity contact described by Bowden and Tabor [13]. The maximum load applied to the crystal was 50 g (the corresponding

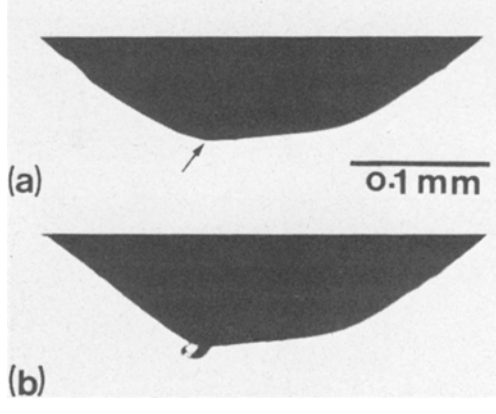

Figure 8 (a) Part of an RDX crystal which did not exhibit any sharp edges. It was loaded at the region marked with the arrow. (b) After loading to 41 g, a thin sliver of the crystal appears to be on the point of detaching when the crystal was separated from the glass plate.

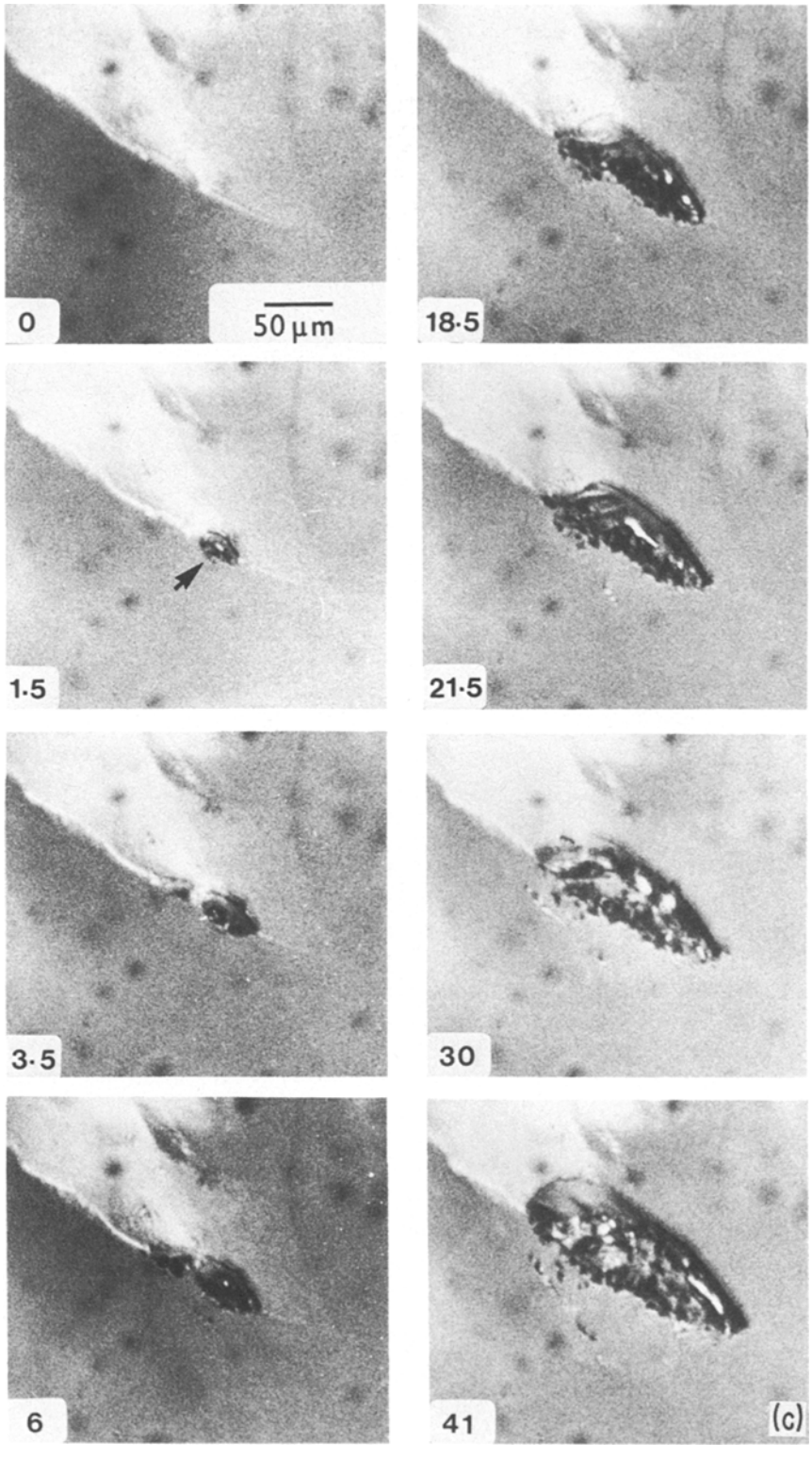

Figure 8 (c) The variation of the area of real contact of the RDX crystal shown in Fig. 8a when it is pressed against the glass plate at different loads. The load (in g) on the crystal is shown at the bottom left-hand corner of each frame. Dark areas represent the real contact.

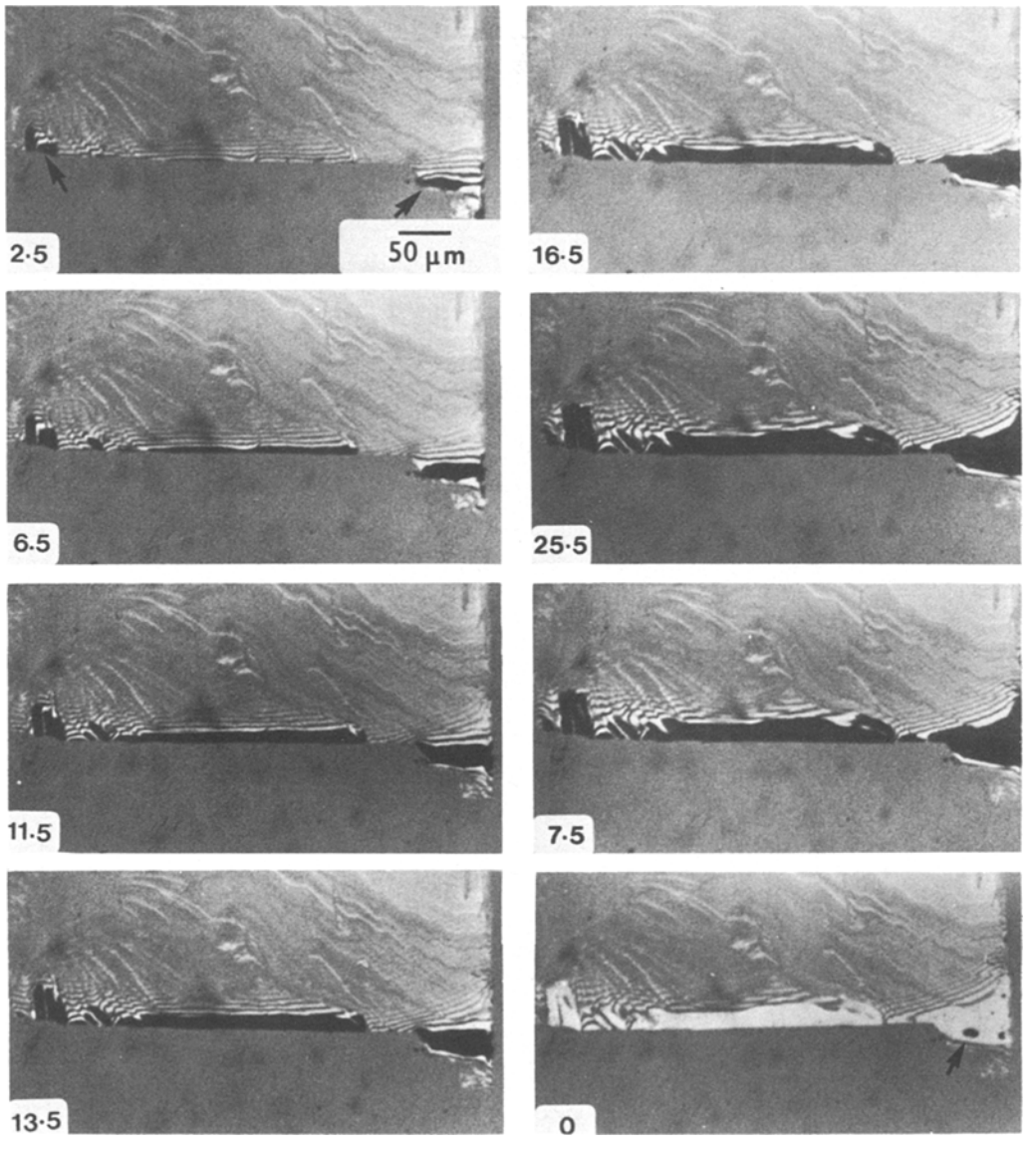

Figure 9 The variation of the area of real contact of a wedge-like crystal of KCl when it was compressed along [1 1 0] against the glass surface at different loads. The load (in g) is shown at the bottom left-hand corner of each frame. Dark areas represent the real contact. Note also the interference fringes; these correspond to regions outside the real contact.

area of real contact is not shown here) and then it was unloaded and again a very thin layer of extremely small particles was left adhering to the glass plate. A photograph of the crystal after the deformation is shown in Fig. 8b. It appears that a thin sliver of the crystal was in the process of being torn off at the contact zone.

3.5. KCl

Fig. 9 shows the variation of the real area of contact for a single crystal of KCl loaded on a fresh edge formed by cleaving along {1 0 0} planes; the direction of compression was approximately along [1 1 0]. (Note that it is because of the lighting conditions that in the figure only one of the {1 0 0} faces forming the edge is seen.) In the first frame, the load is 2.5 g and real contact occurs at isolated points marked by the arrows; interference fringes are also clearly visible outside the real contact zone. As the load is increased, the number of zones in real contact and their areas increase, but no cracking of the crystal occurs. The load was

increased to 25.5 g and then the crystal was unloaded. Note that until the load has dropped to zero there is no significant reduction in the area of real contact (see the frame corresponding to 7.5 g). This strongly suggests that real area of contact is formed by plastically deformed area of the material. Naturally, as the load is decreased, the area of the plastically deformed flat will not reduce. When the load is reduced to zero and the surfaces are just separated, the plastically flowed material gives enhanced illumination. In the last frame (i.e. zero load) a very small zone is still in contact (dark zone marked with arrow); this dark zone also changed to a bright one on further separation. For this crystal no layer of transferred material was left on the glass plate.

4. Data reduction

The average contact stress was obtained by dividing the applied load by the corresponding measured area of real contact. As in all cases, even at the smallest loads studied, plastic deformation of the material had occurred over the entire contact zone, the average contact stress gives us the plastic deformation stress of the material. The variation of the deformation stress with load of the different crystals are shown in Figs. 10 to 14. Except for KCl, all crystals studied show that the deformation stress increases with load, reaching a plateau at higher loads. For crystals of different materials the average deformation stress at high loads was greater by a factor in the range 1.5 to 5.0 than that at low loads. Notice, however, that

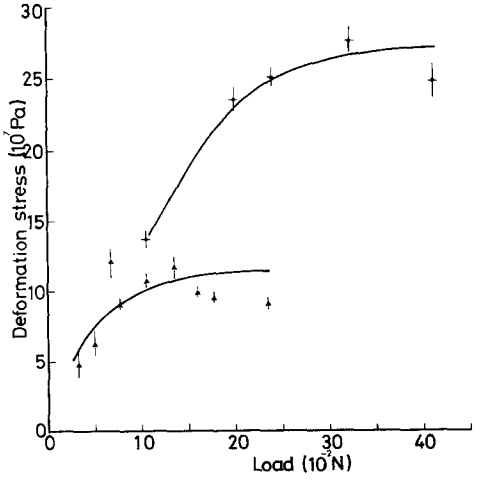

Figure 10 The variation of the deformation stress of α-lead azide crystals with load. •, crystal No. 1; ▲, crystal No. 2.

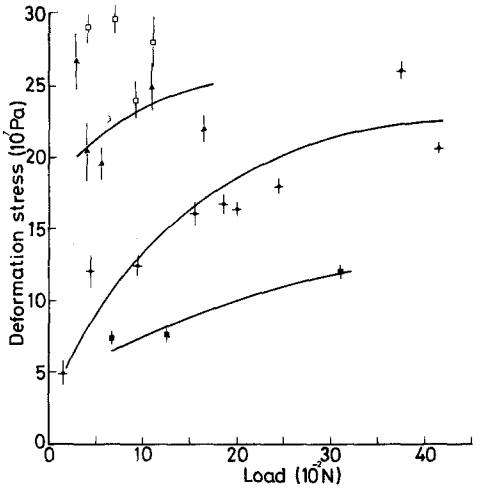

Figure 11 The variation of the deformation stress of LAT type C and type A single crystals with load. •, ▲, □, LAT type C crystal Nos. 1, 2 and 3 respectively; ■, LAT type A single crystal.

deformation stress against load graphs show irreproducible behaviour even for crystals of the same material. Several factors may contribute towards this irreproducibility: (i) a change of the loading axis of the crystal; (ii) a change in the geometry of the loaded region; and (iii) changes in the physical properties from crystal to crystal due to the impurity content variations.

For the case of α-lead azide results from experiments on two crystals are shown (Fig. 10). For one crystal the deformation stress increases from 13×10^7 Pa to 26×10^7 Pa as the load increases from about 10^{-1} N to 4×10^{-1} N, whereas for the second crystal the deformation stress increases from 5×10^7 Pa to 10×10^7 Pa with the increase of load from 4×10^{-2} N to 2×10^{-1} N. The results for three crystals of LAT type C and one of LAT type A are shown in Fig. 11. Crystal No. 1 shows an increase of deformation stress of over four times (i.e., from $\sim 5 \times 10^7$ Pa to 22×10^7 Pa) as the load goes up from 2×10^{-2} N to 40×10^{-2} N. However, in the other two crystals the variation of the deformation stress is not so marked; crystal No. 2 shows an increase of only 25% in the deformation stress, and from the small number of data points (four only) covering a relatively small load range (4 to 10×10^{-2} N) for crystal No. 3, very little variation seems to occur.

In β-HMX crystals (Fig. 12) the variation of the deformation stress with load is from 25% (crystal No. 1) to a factor of 2 (crystal No. 2), though the load range of crystal No. 2 is considerably larger.

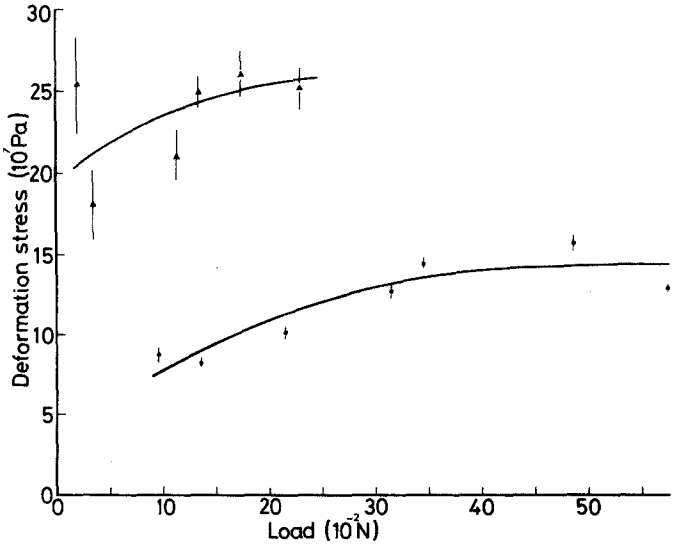

Figure 12 The variation of the deformation stress of β-HMX single crystals with load. ▲, crystal No. 1; ●, crystal No. 2.

One significant difference is the value of the stress at low loads; the deformation stress of one crystal is 3 to 4 times that of the other. In this case it does appear that the geometry of the contact is playing an important part; the lower stress values are for the slightly rounded crystal.

RDX crystals (Fig. 13) also show an increase in the value of the deformation stress by a factor of 2, as the load is increased from 2×10^{-2} N to 40×10^{-2} N. However, as for the other materials, there is a difference in the stress values of one crystal from that of the other.

For the KCl crystal (Fig. 14) the deformation stress remains constant at 2.7×10^7 Pa as the load increases from 4×10^{-2} N to 25×10^{-2} N.

It may be pointed out that for all the crystals studied, the size of the plastically deformed zone at the contact was not more than 1/50th of the size of the crystal. In other words, the plastic deformation was very localized.

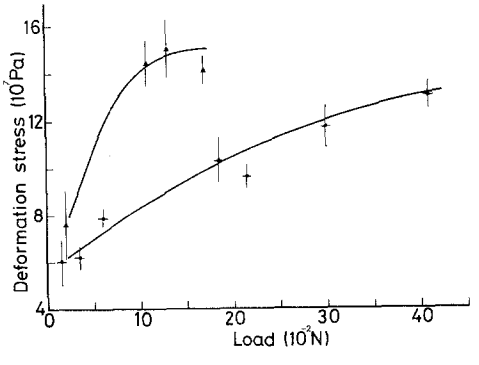

Figure 13 The variation of the deformation stress of RDX single crystals with load. ●, crystal No. 1; ▲, crystal No. 2.

5. Discussion

From the analysis of the data given in Section 4, several important observations can be made regarding the flow stresses of small (mm-size) single crystals of a number of brittle materials:

1. plastic flow occurs even for loads as small as 0.02 N;

2. generally, the flow stress increases with the applied load reaching a plateau at loads of 10^{-1} to 2×10^{-1} N;

3. the maximum deformation stress of a crystal is considerably smaller than its Vickers diamond hardness value (see Table II);

4. except for KCl, all crystals studied leave a film (composed of extremely small particles) on the glass surface against which they are compressed, even for loads as small as 10^{-2} N.

We shall discuss these observations separately.

5.1. Plastic flow at very low loads

The crystals used were as-grown and it is very likely

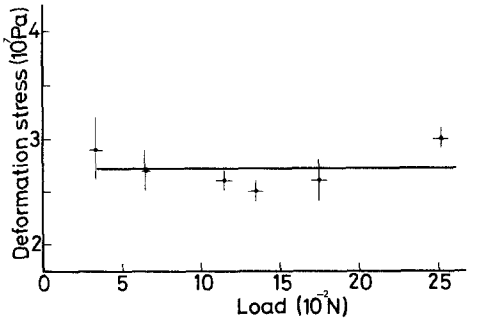

Figure 14 The variation of the deformation stress of a KCl single crystal with load.

that their mechanical behaviour would be that of non-work-hardened crystals. In fact, using the technique of indentation with a hard sphere, it has been found that the crystals of β-HMX and RDX show a considerable amount of work hardening. Now since some of the crystals possess "point-like" corners and some have "line-like" edges, the elastic limit will be exceeded at extremely low loads. This has been confirmed by the experimental observations reported in Section 3.

5.2. The increase of the deformation stress with load

The increase of the deformation stress with load is a little difficult to explain fully for conical, pyramidal and wedge-shaped crystals. It may be possible that a very limited number of slip systems available in these crystals is a contributory factor. It should be pointed out that in the case of cones and wedges of an isotropic material possessing more than five independent slip systems, such as in copper, the deformation stress is independent of the load for the fully work-hardened state and only increases by about 6% when the copper is annealed [14]. Therefore, for the brittle crystals studied, it is reasonable to assume that the work hardening effects will show some increase in the deformation stress with the increase of load. However, more experimental work is needed on other brittle crystals before almost a 100% increase in the deformation stress (see Figs. 10 to 13) with load can be understood.

For crystals whose loading edges were curved (e.g. RDX), the deformation stress against load behaviour is somewhat similar to that of an annealed metallic sphere; in both cases the stress initially increases with load, reaching a peak at higher loads. On comparison with the results from metallic spheres [15], it appears that the initial yield in the crystal occurs at a value only just a few per cent higher than its uniaxial yield stress. The increase of the deformation stress with load can then be explained by the work hardening of the crystal.

5.3. The maximum deformation stress of a crystal against its Vickers diamond hardness

The maximum deformation stress and Vickers diamond hardness of the various crystals are compared in Table II. It is noted that in all cases the latter is considerably higher. Two factors responsible for the difference are:

(i) the constraint imposed on a solid when a Vickers diamond pyramid is pushed into the solid is greater than when a corner or an edge of the solid is pressed against a hard flat surface; and

(ii) the average plastic strain induced by the Vickers diamond pyramid indentation is 8%, whereas the strain induced due to the plastic deformation of a sharp-edged or pointed particle is dependent upon the included angle of the loaded zone, as has been shown for the case of annealed copper cones [14].

One important implication of these findings is that to predict the real area of contact of a brittle particle loaded against a hard flat surface using its Vickers diamond hardness value, as has been done by the previous investigators, is not generally correct; this approach gives very much an underestimate.

5.4. The layer left on the glass plate

Except for KCl, all crystals left a layer of microscopic particles on the glass plate even when compressed by as low a load as 1 g. There appear to be two possible explanations:

(i) the crystals break up due to the compression; and

TABLE II Comparison of maximum deformation pressure of a particle and its Vickers diamond hardness

Material	Vickers diamond hardness* H_V (kg mm^{-2})	Maximum deformation pressure of particle P_m (kg mm^{-2})†	P_m/H_V
α-lead azide (PbN_6)	119.7 ± 8.1	27.5	0.23
RDX	24.1 ± 0.8	15	0.62
β-HMX	41.3 ± 1.0	26	0.63
LAT (type C)	109.4 ± 3.1	29	0.27
LAT (type A)	34.5 ± 0.9	12	0.35
KCl	16 ± 1	2.8	0.18

*Load on indentor was 15 g.
†Error ≈ 5%.

TABLE III Predicted minimum loads for compression cracking

Materials (all single crystals)	Predicted minimum* load for cracking (N)
α-lead azide	6.6×10^{-6}
RDX	1.2×10^{-3}
KCl	1.9×10^{-2}

*Calculated using H_V values.

(ii) the break up does not occur during the compression, but the adhesion between the crystal and the glass surface is so high that when the crystal is separated from the glass, fracture occurs within the crystal.

According to Hagan [16], the critical load P_{cr} to cause cracking of a brittle particle by compression is given by:

$$P_{cr} \simeq 880(K_{IC}/H_V)^3 K_{IC} \quad (3)$$

where K_{IC} is the critical stress intensity factor of the particle and H_V its Vickers diamond pyramid hardness. For plane strain conditions, $K_{IC} = [(2\gamma E)/(1-\nu^2)]^{1/2}$ where γ is the fracture surface energy, E the Young's modulus, and ν the Poisson's ratio. The critical calculated loads to cause cracking are shown in Table III.

It will be seen from Table III that the crystals of PbN_6, RDX and KCl should crack at the loads used in these experiments. It was pointed out above that the deformation pressures of the various crystals are considerably smaller than their Vickers hardness values (Table II). Therefore, if we use the maximum deformation pressures in Equation 3 in place of H_V, the predicted loads will be markedly higher, though both lead azide and RDX will still crack, but not KCl, for the loads employed here.

It must be pointed out that *in situ* observations of the explosive crystals did not show any cracking, suggesting that the adhered layer on the glass probably forms during the unloading (i.e. separation). However, irrespective of the fact whether cracking occurs during loading or unloading, the measurement of the area of real contact will not be affected.

The fact that when a particle of an explosive material comes into contact with a solid surface (e.g. a container), it leaves a thin layer of the explosive on the solid, means that the situation can be hazardous. Therefore, it is important to clean the surface of the container thoroughly after it has been in contact with an explosive, especially if it is of a primary type.

5.5. Flow stress determination

From the deformation stress values of a brittle particle, an estimate of its flow stress (i.e. yield stress at the imposed strain) can be made. If the particle is spherical, then the deformation stress at low loads will correspond closely to the uniaxial yield stress of the explosive crystals used in this work. The values are:

$$\alpha\text{-}PbN_6 \leqslant 5 \times 10^7 \text{ Pa};$$

$$\text{LAT type C} \leqslant 5 \times 10^7 \text{ Pa};$$

$$\text{LAT type A} \leqslant 6.5 \times 10^7 \text{ Pa};$$

$$\beta\text{-HMX} \leqslant 7.5 \times 10^7 \text{ Pa};$$

$$\text{RDX} \leqslant 4 \times 10^7 \text{ Pa}.$$

6. Conclusions

The plastic deformation stress of as-grown single crystals of a number of explosive materials has been successfully determined using a new experimental technique. The experiments involved measuring the real area of contact between the test crystal and a transparent glass plate pressed together with a given normal load. The deformation stress was found to increase with load, reaching a plateau at higher loads. It was discussed whether the plastic deformation stress of a particle approaches its uniaxial yield stress at low normal loads; estimates of the limiting values of the uniaxial yield stress of the explosive crystals have been given.

Acknowledgements

The author should like to thank Drs J. T. Hagan and E. H. Yoffe for comments on the manuscript, Dr P. H. Collins (PERME) for supplying the LAT crystals, and Dr J. E. Field and Mr S. J. P. Palmer for discussions on β-HMX crystals. The work was supported in part by the Ministry of Defence (Procurement Executive) and in part by the US Government through its European Research Office.

References

1. M. M. CHAUDHRI, *Nature* **263** (1976) 121.
2. D. TABOR, *J. Lub. Technol.* **103** (1981) 169.
3. J. T. HAGAN and M. M. CHAUDHRI, *J. Mater. Sci.* **12** (1977) 1055.
4. S. J. P. PALMER and J. E. FIELD, *Proc. Roy. Soc.* **A383** (1982) 399.
5. M. M. CHAUDHRI, PhD Thesis, University of Cambridge (1969).
6. C. S. CHOI and H. P. BOUTIN, *Acta Crystallogr.* **B25** (1969) 982.

7. MELANIE A. PIERCE-BUTLER, *ibid.* **B38** (1982) 2681.
8. H. H.CADY, A. C. LARSON and D. T. CROMER, *ibid.* **16** (1963) 617.
9. C. S. CHOI and E. PRINCE, *ibid.* **B28** (1972) 2857.
10. P. J. HALFPENNY, K. J. ROBERTS and J. N. SHERWOOD, *J. Mater. Sci.* **19** (1984) 1629.
11. H. D. MEGAW, "Crystal structures: A Working Approach" (Saunders Company, London, 1973) p. 82.
12. M. T. SPRACKLING, "The Plastic Deformation of Simple Ionic Crystals" (Academic Press, London, 1976) p. 23.
13. F. P. BOWDEN and D. TABOR, "The Friction and Lubrication of Solids" (Clarendon Press, Oxford, 1950) p. 5.
14. M. M. CHAUDHRI, *Phil. Mag.* **A48** (1983) L15.
15. M. M. CHAUDHRI, I. M. HUTCHINGS and P. L. MAKIN, *ibid.* **A49** (1984) 493.
16. J. T. HAGAN, *J. Mater. Sci. Lett.* **16** (1981) 2909.

Received 24 November
and accepted 29 November 1983